ACADEMIC PRESS

Journal of Solid State Chemistry 169 (2002) 176–181

JOURNAL OF SOLID STATE CHEMISTRY

www.academicpress.com

Crystallography and crystallite morphology of rutile synthesized at low temperature

X. Bokhimi,[a,*] A. Morales,[a] and F. Pedraza[b]

[a] *Institute of Physics, The National University of Mexico (UNAM), A.P. 20-364, 01000 México D.F., Mexico*

[b] *Molecular Engineering Program, Instituto Mexicano del Petróleo, Eje Central L. Cárdenas 152, A.P. 14-805, 07730 México D.F., Mexico*

Received 3 June 2002; received in revised form 30 August 2002; accepted 12 September 2002

Abstract

Rutile was prepared at low temperature with titanium trichloride in an acid- and oxygen-rich environment. Samples were characterized with X-ray powder diffraction, transmission electron microscopy, and thermogravimetry; rutile's crystalline structure was refined with the Rietveld method. Crystallites were needles with their largest dimension along *c* lattice parameter; they grew in bundles parallel to their length axis, and contained hydroxyls in their lattice and on their surface. When samples were annealed, dehydroxylation generated lattice defects that produced microstrains and created conditions for crystallite sintering at temperatures above 300°C. Titanium–oxygen interaction in rutile depended on the annealing temperature, which gave rise to changes in the symmetry of the representative rutile titanium–oxygen octahedron. The atomic bond length between the oxygen atoms shared by adjacent octahedra decreased with the temperature, contracting the lattice. All this was caused by the variation of the number of hydroxyls in the lattice.

Keywords: Nanocrystalline rutile; Low temperature synthesis; Lattice defects; Crystallite sintering; Hydroxyls in lattice; Atomic bond lengths

1. Introduction

Titania is an oxide widely used in electronics [1–3], catalysis [4–6], coating [7–9], and in medicine [10,11]. Its properties depend on the atom distribution in its phases, because titania can have several polymorphs [12], from which rutile is the most stable at normal conditions [13]; at high pressures there are other more stable titania phases [14–17]. At normal conditions, in general, rutile is obtained from the transformation of the other titania phases, anatase and brookite, after their annealing above 400°C [18]. Rutile is also obtained from titanium solutions [19], when seeds of oxides with the rutile-type structure are embedded into it; for example, seeds of SnO_2. Recently, however, rutile has been synthesized at low temperature via soft chemistry [18,20–24].

This titania polymorph is synthesized at room temperature by using the sol–gel method with titanium ethoxide as precursor and HCl functioning only as hydrolysis catalyst in the synthesis [18]. In this way, its concentration in the fresh sample is small, and the average crystallite size a little large, 35(1) nm; it coexisted with anatase, the main phase, and brookite. When titania is prepared in acidic conditions and in the presence of platinum with titanium buthoxide as precursor, the amount of rutile in the fresh sample increases considerably [20], being the main phase in the sample. In this case, it was assumed that platinum caused this increase of rutile concentration; the acidic conditions, however, were not taken into account to explain it. New reports in the literature [22–24] and our search for titania nanotubes show that rutile is produced at low temperature as an effect of the acidic conditions used in the synthesis.

This titanium polymorph can also be synthesized at low temperature by using titanium trichloride as precursor [21], and from titanium tetrachloride dissolved in aqueous solutions of HCl, HNO_3 or H_2SO_4 [24], which gives rise to a crystallite size between 20 and 50 nm. During our search for getting titania nanotubes using titanium alkoxide as titanium precursor in an

*Corresponding author. Fax: +52-562-250-08.

E-mail address: bokhimi@fisica.unam.mx (X. Bokhimi).

0022-4596/02/$ - see front matter © 2002 Elsevier Science (USA). All rights reserved.
PII: S0022-4596(02)00046-4

acidic solution made with HCl, we also got rutile at low temperature, with crystallites smaller than the ones reported for the synthesis methods described above.

The crystallite size of the rutile prepared at low temperature increases when the sample is annealed [13]. A quantitative analysis of the crystallography changes that occur when the sample is annealed, however, has not been performed, although these changes in the atom distribution determine many of the rutile's properties.

Recently, it was shown that in nanocrystalline boehmite the atomic interactions and the local symmetry depend on the crystallite size [25–26]. Therefore, it is of interest, to analyze the corresponding behavior of the nanocrystalline rutile prepared at low temperature, in order to know if in this nanocrystalline system the atomic interactions depend on the crystallite size too. This information will be very helpful to those interested in interpreting the properties of rutile measured by using different techniques, when it is sintered at low temperature.

In the present work, we analyze the evolution as a function of the sample annealing temperature, of the crystallography, crystallite size, and microstrains of rutile prepared at low temperature with titanium trichloride as precursor. This was performed by refining rutile's crystalline structure via Rietveld method, starting from X-ray powder diffraction patterns measured at room temperature. Samples were also analyzed with transmission electron microscopy (TEM) and thermogravimetry.

2. Experimental

2.1. Sample preparation

According to Ref. [21], rutile was prepared from titanium trichloride (Fluka, 15 wt% in hydrochloric acid), which was dissolved in deionized water at room temperature. This solution was stirred continuously in contact with atmospheric oxygen for 60 h; its pH was adjusted to 1.0 with HCl. The white precipitate was filtered, and dried at 100°C for 15 h (fresh sample). This sample was annealed in air for 12 h at 150°C, 200°C, 300°C, 400°C, 500°C, 600°C, 700°C, 800°C, 900°C, 1000°C and 1080°C. After each annealing, the sample was analyzed with X-ray powder diffraction; a portion of it was separated for the analysis with TEM.

2.2. Sample characterization

2.2.1. X-ray diffraction

The X-ray diffraction pattern of the sample packed in a glass holder was recorded at room temperature with Cu$K\alpha$ radiation in a Bruker Advance D-8 diffractometer that had $\theta-\theta$ configuration and a graphite monochromator in the secondary beam. Diffraction intensity was measured between 10° and 110°, with a 2θ step of 0.02° for 2.5 s per point. Crystalline structure was refined with the Rietveld technique by using FULLPROF98 code (J. Rodríguez-Carbajal, Laboratoire Leon Brillouin (CEA-CNRS), France Tel.: (33)-1-6908-3343; Fax: (33)-1-6908-8261, E-mail: juan@llb.saclay.cea.fr); peak profiles modeled with pseudo-Voigt functions [27] contained average crystallite size and microstrain as two of the characteristic parameters [28]: The effect of the microstrain was included in the Gaussian portion of the function, while the corresponding effect of the size was included in the Lorentzian portion. The concentration of titanium vacancies was determined by refining its occupation number. Thermal vibration parameters for atoms were also refined; they were always positive, taking values around 0.5 for titanium atoms and around 1.0 for oxygen atoms. Standard deviations, which show the last figure variation of a number, are given in parentheses. When they correspond to refined parameters, their values are not estimates of the probable error in the analysis as a whole, but only of the minimum possible probable errors based on their normal distribution [29].

2.2.2. Thermoanalysis

Weight losses and the temperatures associated to phase transformations were determined by thermogravimetry with a Perkin-Elmer TG-7 apparatus; samples were heated from room temperature up to 1000°C at 10°C/min.

2.2.3. Transmission electron microscopy (TEM)

The samples, milled and dispersed in ethanol before their supporting in the copper grid covered with formvar, were observed at 200,000× with a Jeol 100C× transmission electron microscope that had high-resolution polar pieces.

3. Results and discussion

In all samples we always found only one phase, rutile (Fig. 1). Its crystalline structure was refined with a tetragonal unit cell that had the symmetry described by space group $P4_2/mnm$ and the atom positions given in Table 1. According to this table, titanium atom position is fixed in unit cell, while oxygen atom have variable x and y coordinates, which allows distortion of the octahedra formed with titanium atom in its center and oxygen atoms in the corners. Fig. 2 shows a typical Rietveld refinement plot.

For the refinement, in the starting model, it was assumed that crystallite shape was spherical. This, however, caused that the intensity of the calculated (110) reflection was larger than the experimental one,

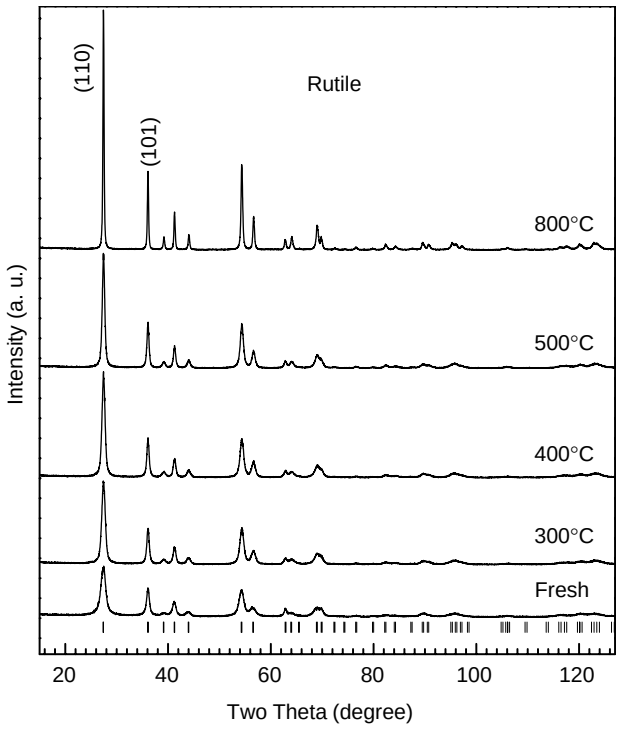

Fig. 1. X-ray diffraction pattern of the sample annealed at different temperatures. The tick marks and Miller indices correspond to rutile.

Table 1
Rutile, space group $P4_2/mnm$ (136): Atom positions

Atom	Site	x	y	z
Ti	2*a*	0.0	0.0	0.0
O	4*f*	*u*	*u*	0.0

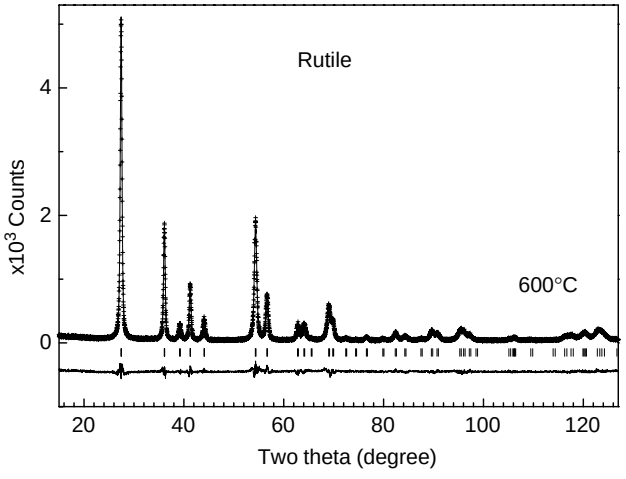

Fig. 2. Rietveld refinement plot of the sample annealed at 600°C ($R_{wp} = 0.156$, $R_F = 0.038$). Crosses correspond to the experimental data; continuous line, to the calculated ones, and the difference between experimental and calculated data. Tick marks correspond to rutile.

while the calculated intensity of the (101) reflection had a lower intensity than the one obtained in the experiment (Fig. 1). Besides, the assumed spherical shape of the crystallites also gave rise to a peak width for the (110) reflection smaller than the one got from the experiment, and to a larger width for the calculated (101) peak than the one observed in the measured data. This result pointed out for an anisotropic crystallite shape, which was confirmed with the analysis of the samples by using TEM (Fig. 3).

The anisotropy of the crystallite shape was modeled by assuming that crystallites had a needle-like form with the needle axis parallel to [001] direction, along which titanium–oxygen octahedra share one edge, forming octahedra filaments (Fig. 4 and Ref. [13]). With this new model, the calculated data fitted better to the experiment (Fig. 2).

After synthesis, 4 wt% of the sample corresponded to water that was desorbed below 100°C (Fig. 5). Between 100°C and 300°C, the sample had another weight loss of 4.5 wt% caused by dehydroxylation. Finally, the sample lost 1.09% of its weight when it was annealed from 300°C to 700°C. This last weight loss was related to the sintering of the crystallites, as it will be shown below from the X-ray powder diffraction and the TEM studies.

The dehydratation and dehydroxylation of the sample observed below 300°C (Table 2), gave rise to a microstrain $\langle \varepsilon \rangle$ produced by the fact that unit cells are similar but they are not identical. This microstrain was maximal when the sample was annealed at 300°C, suggesting that the hydroxyls were not only on crystallite surface but also in its bulk, because they gave rise to defective unit cells when left sample's bulk. This microstrain decreased monotonously when the sample was annealed at higher temperatures as an effect of the continuous dehydroxylation and atom diffusion. The model for the microstrain we used was simple, because it was assumed isotropic. It is, however, a first approximation that would be improved when more studies will be performed in this system to have a better understanding of it.

The hydroxyls in rutile lattice explain not only the presence of the microstrains, but also of the large cation deficiency observed during the refinement (Table 3): It was 16.0(8)% in the fresh sample and only 10.4(8)% when sample was annealed at 400°C. These defects are the more direct evidence of the presence of hydroxyls in the lattice, because only with them it is possible to compensate the large charge difference. From the refinement, it is inferred that the oxygen atom of hydroxyls should be in the sites corresponding to the oxygen position given in Table 3. Since hydrogen atoms scatter X rays weakly, they do not contribute significantly to the diffraction pattern, and were not considered in the model for the refinement.

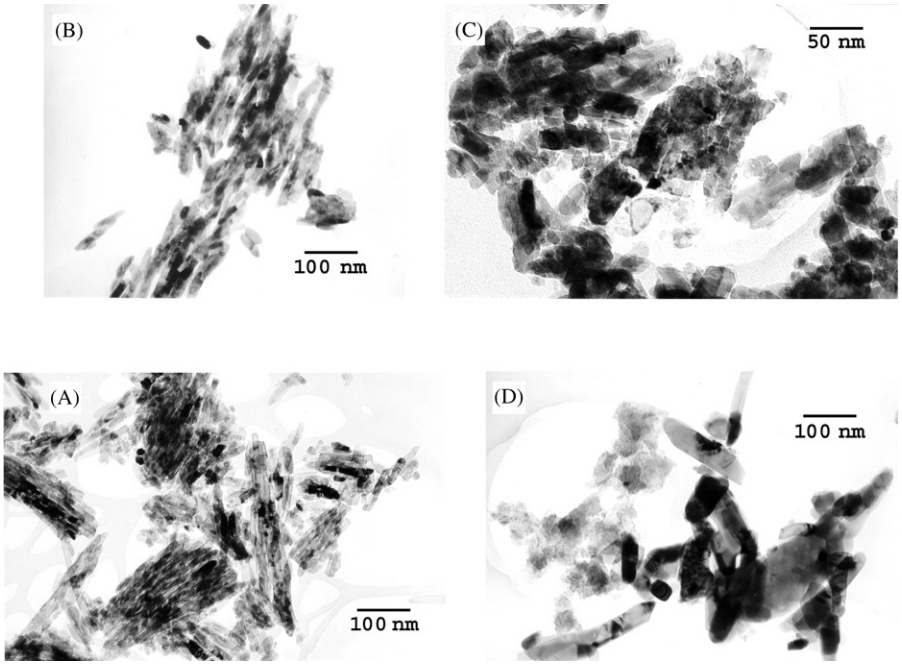

Fig. 3. Transmission electron micrographs taken at 200,000× of the sample annealed at different temperatures: (A) 300°C, (B) 400°C, (C) 500°C, and (D) 800°C.

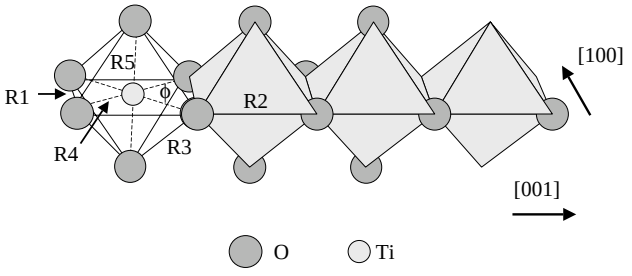

Fig. 4. Rutile's crystalline structure, showing the filaments that form titanium–oxygen octahedra sharing edges. The different atomic bond lengths, and one of the representative angles, ϕ, of its crystalline structure are indicated.

Table 2
Microstrain $\langle\varepsilon\rangle$, crystallite diameter D and length L

T (°C)	$\langle\varepsilon\rangle$ (%)	D (nm)	L (nm)	L/D
Fresh	1.65(9)	9.0(3)	>400	>44
150	1.80(9)	9.2(3)	>400	>43
200	2.02(9)	10.7(3)	>400	>37
300	2.17(7)	15.1(6)	>400	>26
400	2.07(6)	18.4(8)	>400	>21
500	1.80(5)	22(1)	138(52)	6(2)
600	1.44(6)	32(2)	131(10)	4.1(3)
700	1.12(2)	44(2)	89(10)	2.0(2)
800	0.90(2)	58(4)	104(12)	1.8(2)
900	0.74(2)	74(5)	124(15)	1.7(2)
1000	0.44(1)	100(9)	157(21)	1.6(2)
1080	0.21(1)	143(10)	219(23)	1.5(2)

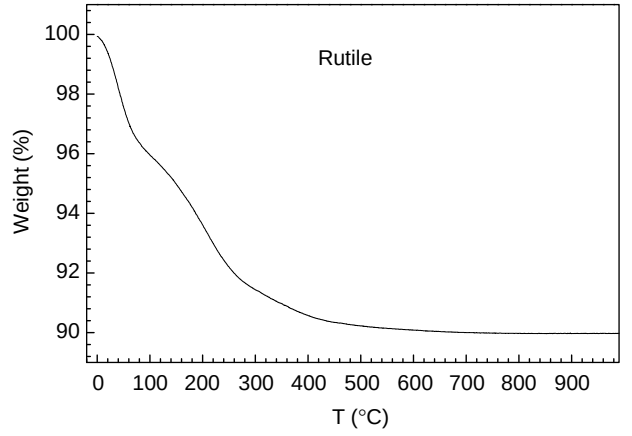

Fig. 5. Thermogravimetric curve when the sample was annealed in air at 10°C/min.

Table 3
Lattice parameters a and c, oxygen u coordinate, O_x, titanium vacancy, and unit-cell volume

T (°C)	a (nm)	c (nm)	O_x	Ti Vacancy (%)	Volume (nm^3)
Fresh	0.46021(4)	0.29563(2)	0.3025(3)	16.0(8)	0.06261(2)
150	0.46006(4)	0.29567(2)	0.3015(3)	15.2(8)	0.06258(2)
200	0.45977(4)	0.29564(2)	0.3023(3)	13.6(8)	0.06249(2)
300	0.45945(3)	0.29565(2)	0.3032(3)	12.0(8)	0.06241(1)
400	0.45935(3)	0.29566(2)	0.3035(3)	10.4(8)	0.06243(1)
500	0.45931(3)	0.29568(2)	0.3037(3)	10.4(8)	0.06238(1)
600	0.45927(2)	0.29569(1)	0.3042(3)	10.4(8)	0.06237(1)
700	0.45927(1)	0.29575(1)	0.3045(3)	9.6(8)	0.06238(1)
800	0.45925(1)	0.295741(8)	0.3042(3)	9.6(8)	0.06237(1)
900	0.45921(1)	0.295740(7)	0.3045(3)	9.6(8)	0.06236(1)
1000	0.459257(8)	0.295774(6)	0.3044(3)	8.8(8)	0.06238(1)
1080	0.459248(5)	0.295789(4)	0.3062(3)	8.8(8)	0.06238(1)

After synthesis, the rutile needle-like crystallites, with needle diameters lower than 10 nm and lengths larger than 400 nm (Table 2), formed bundles of crystallites parallel to the needle axis (Fig. 3A), in as similar way as those reported for dihydrate titanyl sulfate [30]. Their diameter was probably limited by the large amount of hydroxyls in the lattice, which produced defects that hindered atomic order at large distances along it. Since crystallites largest dimension was along *c*-axis, and titanium–oxygen octahedra share oxygen atoms along *a*-axis, hydroxyls should be mainly in the apical positions, which correspond to the atomic bond length *R*5 (Fig. 4).

As the annealing temperature was increased, crystallite diameter increased while its length diminished (for annealing temperatures lower than 800°C), decreasing with that the magnitude of the anisotropy, which in the present case was measured by the ratio between the needle length (L) and its diameter (D), both determined from the refinement (Table 2).

The increase of crystallite diameter, when the annealing temperature was risen, suggests that neighboring crystallites sintered between each other (Fig. 3 and Table 2); this sintering followed the dehydroxylation below 300°C, and was associated with the sample weight loss observed between 300°C and 700°C. At 400°C the sintering was between two adjacent crystallites (Table 2), while at 600°C, it covered three crystallites; at 800°C, in an average, more than five neighboring crystallites were sintered, building very compact cylinders (Fig. 3D). At the highest annealing temperature, 1080°C, the L/D ratio was only 1.5(2). Since adjacent crystallites were not necessarily parallel, the atomic diffusion caused breaking of the atomic order along *c*-axis, decreasing with that the domain coherence along this direction, as it was determined from the refinement (Table 2).

Prior to sintering the sample lost many hydroxyls, causing large microstrains in the crystallites (Table 2); consequently, the number of defects in the sample was large, favoring with that the atom diffusion responsible for the sintering. Since it occurred between adjacent crystallites just after dehydration and dehydroxylation, the space between them after synthesis should be filled with water molecules and hydroxyls, which, during synthesis process, hindered crystallite growing along the directions perpendicular to needle axis.

Since this axis is parallel to [001] direction, i.e., along *c* lattice parameter, crystallite diameter is related to *a*-axis, which should be more sensitive to the above described changes because sintering occurred perpendicular to [001] direction. This explains why the lattice parameter *a* changed more during the annealing than it did the *c* lattice parameter (Table 3). This change of lattice parameter *a*, which, after sintering at high temperatures, had a value similar to the one reported for large crystallites of rutile [31,15], and was caused by the variation of *x* and *y* oxygen atom coordinates in unit cell. These coordinates changed from 0.3025(3) for the fresh sample to 0.3062(3) for the sample annealed at 1080°C (Table 3). The *c* lattice parameter has values slightly smaller than those reported for large crystallites of rutile, 0.29587 [30] and 0.29589(1) [15]. The volume of the unit cell decreased as the annealing temperature was increased; it, however, was constant for temperatures above 500°C. This constant value was smaller than the one reported for large rutile crystallites, 0.06244(1) [31,15]. A decrease of the volume of rutile unit cell has been only observed when it is exposed to high pressure [16].

The change of the oxygen position in unit cell reflects the variation of the Ti–O bonds in lattice (Fig. 4). The atomic bond length (*R*4) that corresponds to the interaction between titanium and the oxygen atoms in the basal plane of the octahedron decreased as the sample annealing temperature was increased (Table 4), while the atomic bond length between titanium and the apical oxygen atoms (*R*5) increased. This happened because the number of titanium vacancies diminished, increasing with that the number of complete titanium–oxygen octahedra sharing edges and having therefore a stronger interaction. It is observed that the octahedron symmetry was larger for the fresh samples, which had a

Table 4
Atomic bond lengths and the atomic bond angle ϕ (Fig. 4)

T (°C)	*R*1 (nm)	*R*2 (nm)	*R*3 (nm)	*R*4 (nm)	*R*5 (nm)	ϕ (deg)	*R*5/*R*4
Fresh	0.25708(7)	0.29563(4)	0.27773(6)	0.19589(5)	0.19688(7)	82.02(2)	1.0051(4)
150	0.25830(7)	0.29567(4)	0.27751(6)	0.19630(5)	0.19616(7)	82.28(2)	0.9993(4)
200	0.25709(7)	0.29564(4)	0.27751(6)	0.19590(5)	0.19556(7)	82.02(2)	0.9983(4)
300	0.25575(7)	0.29565(4)	0.27752(6)	0.19546(7)	0.19701(7)	81.72(2)	1.0079(4)
400	0.25530(7)	0.29566(4)	0.27753(6)	0.19532(5)	0.19716(7)	81.62(2)	1.0094(4)
500	0.25502(7)	0.29568(4)	0.27755(6)	0.19523(5)	0.19727(7)	81.55(2)	1.0104(4)
600	0.25435(7)	0.29569(4)	0.27761(6)	0.19502(5)	0.19758(7)	81.40(2)	1.0131(4)
700	0.25396(7)	0.29575(4)	0.27769(6)	0.19491(5)	0.19778(7)	81.31(2)	1.0147(4)
800	0.25434(7)	0.29574(4)	0.27762(6)	0.19503(5)	0.19757(7)	81.39(2)	1.0130(4)
900	0.25392(7)	0.29574(4)	0.27765(6)	0.19490(5)	0.19775(7)	81.30(2)	1.0146(4)
1000	0.25408(7)	0.29577(4)	0.27766(6)	0.19496(5)	0.19771(7)	81.33(2)	1.0141(4)
1080	0.25174(7)	0.29579(4)	0.27797(6)	0.19421(5)	0.19887(7)	80.80(2)	1.0234(4)

larger angle ϕ formed in the basal plane by the interaction between titanium atom and the oxygen atoms of the edge shared by contiguous octahedra. This reflects a weakening of the preferential interaction between neighboring octahedra, characteristic of rutile, caused by the presence of a large number of octahedra without the titanium atom in their center.

The basal plane of the representative octahedron was also deformed when the sample annealing temperature was increased: The angle ϕ representative of this plane varied from 82.02(2)° for the fresh sample to 80.80(2)° for the one annealed at 1080°C. Although the Ti–O oxygen interactions in plane was the same for all oxygen atoms, the oxygen–oxygen atomic bond length ($R1$) of the oxygen atoms shared with adjacent octahedra decreased as the annealing temperature was increased. It varied from 0.25708(7) nm for the fresh sample to 0.25174(7) nm for the sample annealed at 1080°C. The shortening of this length as the annealing temperature was increased gave rise to the observed contraction of the lattice (Table 2). At it was noticed before, the weakness of this interaction in the samples annealed at low temperature was caused by the presence of many titanium vacancies, i.e. to the large amount of octahedra without the titanium atom in their center.

4. Conclusions

The rutile prepared at low temperature with titanium trichloride as precursor contained hydroxyls in its lattice and around the crystallites, which were needles with their largest dimension oriented along c lattice parameter. Crystallites grew in bundles parallel to their length axis. When samples were annealed, the dehydroxylation generated lattice defects that produced microstrains and created conditions for crystallite sintering at temperatures above 300°C. Titanium–oxygen interaction depended on the annealing temperature, which changed the symmetry of the representative rutile titanium–oxygen octahedron. The atomic bond length between the oxygen atoms shared by adjacent octahedra decreased with the temperature and contracted the lattice. All this was caused by the variation of the number of hydroxyls in the lattice.

Acknowledgments

We would like to thank Eng. M. Aguilar for technical assistance. This work was partially financed with FIES D.00079; FIES-98-23-III project.

References

[1] N. Savage, B. Chwieroth, A. Ginwalla, B.R. Patton, S.A. Akbar, P.K. Dutta, Sensors Actuators B 79 (2001) 17.
[2] G. Phani, G. Tulloch, D. Vittorio, I. Skryabin, Renewable Energy 22 (2001) 303.
[3] M. Watanabe, H. Uchida, Y. Seki, M. Emori, P. Stonehart, J. Electrochem. Soc. 143 (1996) 3847.
[4] K. Fukushima, G.H. Takaoka, J. Matsuo, I. Yamada, Jpn. J. Appl. Phys. I 36 (1997) 813.
[5] M. Najbar, J. Camra, Solid State Ionics 101–103 (1997) 707.
[6] A. Wang, J.G. Edwards, J.A. Davies, Sol. Energy 52 (1994) 459.
[7] W.E. Vargas, P. Greenwood, J.E. Otterstedt, G.A. Niklasson, Sol. Energy 68 (2000) 553.
[8] S. Ono, Y. Nishi, S. Hirano, J. Am. Ceram. Soc. 84 (2001) 3054.
[9] M. Fallet, H. Mahdjoub, B. Gautier, J.-P. Bauer, J. Non-Cryst. Solids 293–295 (2001) 527.
[10] P.A. Ramires, A. Giuffrida, E. Milella, Biomaterials 23 (2002) 397.
[11] A. Stoch, A. Brozek, G. Kmita, J. Stoch, W. Jastrzebski, A. Rakowska, J. Mol. Struct. 596 (2001) 191.
[12] L. Pauling, J.H. Sturdivant, Kryst. Zhidk. 68 (1928) 239.
[13] X. Bokhimi, A. Morales, M. Aguilar, J.A. Toledo-Antonio, F. Pedraza, Int. J. Hydrogen Energy 26 (2001) 1279.
[14] A.E. Goresy, M. Chen, L. Dubrovinsky, P. Gillet, G. Graup, Science 293 (2001) 1467.
[15] L. Gerward, J. Staun Olsen, J. Appl. Crystallogr. 30 (1997) 259.
[16] H. Sato, S. Endo, M. Sugiyama, T. Kikegawa, O. Shimomamura, K. Kusaba, Science 251 (1991) 786.
[17] J. Haines, J.M. Léger, Physica B 192 (1993) 233.
[18] X. Bokhimi, A. Morales, O. Novaro, T. López, E. Sánchez, R. Gómez, J. Mater. Res. 10 (1995) 2788.
[19] J. Zhao, Z. Wang, L. Wang, H. Yang, M. Zhao, J. Mater. Sci. Lett. 17 (1998) 1867.
[20] E. Sánchez, T. López, R. Gómez, X. Bokhimi, A. Morales, O. Novaro, J. Solid State Chem. 122 (1996) 309.
[21] F. Pedraza, A. Vázquez, J. Phys. Chem. Solids 60 (1999) 445.
[22] S.J. Kim, S.D. Park, Y.H. Jeong, J. Am. Ceram. Soc. 82 (1999) 927.
[23] S.T. Aruna, S. Tirosh, A. Zaban, J. Mater. Chem. 10 (2000) 2388.
[24] S. Yin, R. Li, Q. He, T. Sato, Mater. Chem. Phys. 75 (2002) 76.
[25] X. Bokhimi, J.A. Toledo-Antonio, M.L. Guzmán-Castillo, F. Hernández-Beltrán, J. Solid State Chem. 159 (2001) 32.
[26] X. Bokhimi, J.A. Toledo-Antonio, M.L. Guzmán-Castillo, B. Mar-Mar, F. Hernández-Beltrán, J. Navarrete, J. Solid State Chem. 161 (2001) 319.
[27] P. Thompson, D.E. Cox, J.B. Hasting, J. Appl. Crystallogr. 20 (1987) 79.
[28] R.A. Young, P. Desai, Arch. Nauki Mater. 10 (1989) 71.
[29] E. Prince, J. Appl. Crystallogr. 14 (1981) 157.
[30] M.L. Reynolds, T.J. Wiseman, J. Inorg. Nucl. Chem. 29 (1967) 1381.
[31] C.Y. Howard, T.M. Sabine, F. Dickson, Acta Crystallogr. B 47 (1991) 462.